Chapter 2 Principle and design

In the MEMS-based spot scan system, the scanning knife-edge plate is actuated by a comb actuator (Fig 2-1(a)). A right-angle triangular region in the movable part of the comb actuator is used to scan the optical profile in two orthogonal directions. As shown in Figs 2-1(b) to Fig 2-1(d), there are three design and operation modes.

The transmission type (Fig 2-1(b)) is a miniaturization of the traditional system, with a photo detector placed behind the knife-edge plate. The partial optical energy that is not blocked by the MEMS knife-edge plate is detected by the detector. The photo detector and signal processing circuitry are fabricated in one chip; the knife-edge plate and actuators can be fabricated either in the same chip by low temperature post-IC processes such as electroplating, or in another chip which will be bonded with the circuitry chip subsequently.

In the reflection type (Fig 2-1(c)), a triangular reflective area is used as the knife-edge plate. The partial light energy that falls on and reflected from the reflective mirror is detected by a remote photo detector. The comb actuator with reflective mirrors can be fabricated with standard polysilicon surface micromachining techniques, such as MUMPs, and used as a convenient prototyping device.

In the last absorption type (Fig 2-1(d)), a triangular photo detector is directly integrated and vibrates with the comb actuator. The level of integration is higher than the other two types. In this absorption mode, the partial light energy that falls in the area of the detector is absorbed and contributes to the output signal. For high detection sensitivity, photo diodes fabricated in single crystalline silicon substrates such as SOI or <111> silicon should be used. Theoretically speaking, the knife-edge plate itself is the detector so the measurement resolution is only limited by the

position control and detection circuits, not by the spatial resolution of the optical system.

Hence, a high-performance absorption-type system on <111> silicon are designed and fabricated. Additionally, a reflection-type system using MUMPs is also fabricated as a prototype and proof of concept. The design and analysis of the comb drive actuator and the photo detector are discussed in the following.

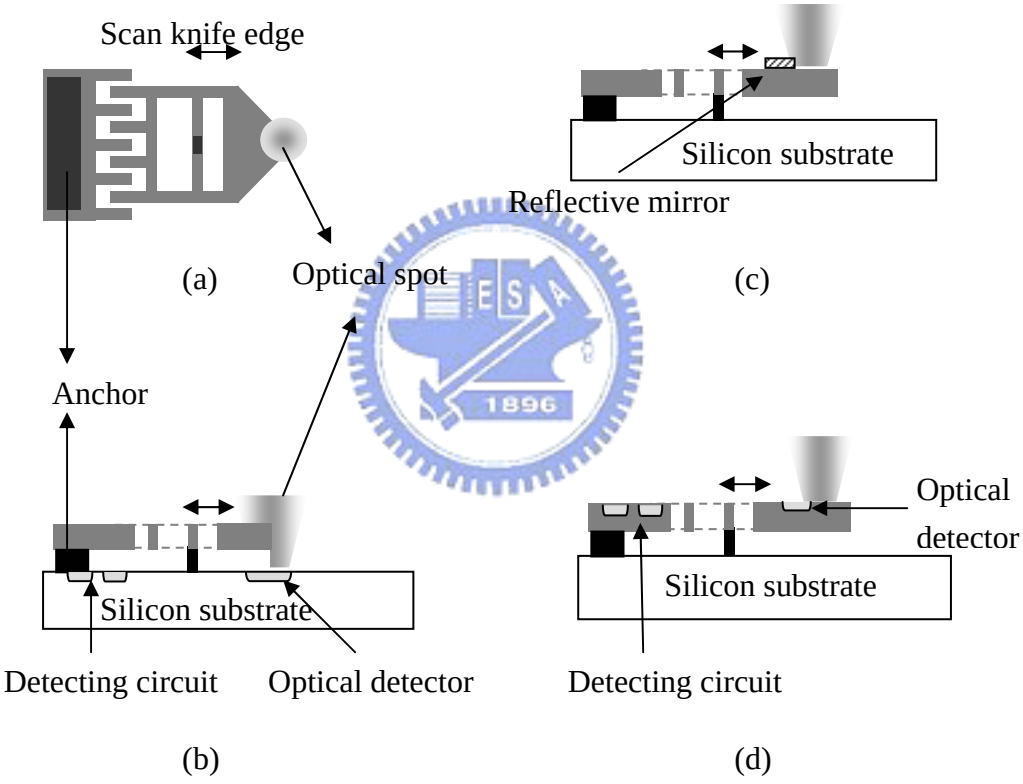

Fig 2-1 MEMS optical spot scanning system, (a) top view, (b) transmission type, (c) reflection type, (d) absorption type

2-1 Comb actuator

In the section, theoretical analysis and finite element modeling (FEM) of static and dynamic characteristics of the comb actuator are presented. A comb actuator consists of two sets of interdigitated finger structures (combs) with one comb fixed and the other connected to an elastic suspension. The movable comb is displaced by the electrostatic force if a voltage difference is applied between the fixed and movable combs. From the balance of the elastic spring force and the electrostatic force, the displacement can be derived.

2-1-1 Spring constant

The spring constant of the elastic structure can be derived from the beam bending equation [14]. For a spring element with pure bending, as shown in Fig 2-2(a), the spring constant in x-direction is:

$$K_x = \frac{F_L}{x} = \frac{Ew_s^3 t}{L^3} \qquad (2\text{-}1)$$

where t represents the thickness of the spring and w_s is the width of the spring, and L is the length of the spring. F_L is the load for the spring and x is the relative displacement of the spring

In a more complex structure as shown in Fig 2-2(b), the total spring constant along the x-direction is four times the serious connection of two springs with length L_{s1} and L_{s1}.

$$K_x = 4\left(\frac{\frac{Etw_s^3}{L_{s1}^3}\times\frac{Etw_s^3}{L_{s2}^3}}{\frac{Etw_s^3}{L_{s1}^3}+\frac{Etw_s^3}{L_{s2}^3}}\right) = 4\frac{Etw_s^3}{L_{s1}^3+L_{s2}^3} \qquad (2\text{-}2)$$

In order to reduce the device layout area and the residual stress effect, a folded structure in Fig 2-2(c) is usually used. In the structure, the beam with length L_{s2} is folded into the inner area and the spring constant is the same with Eq (2-2).

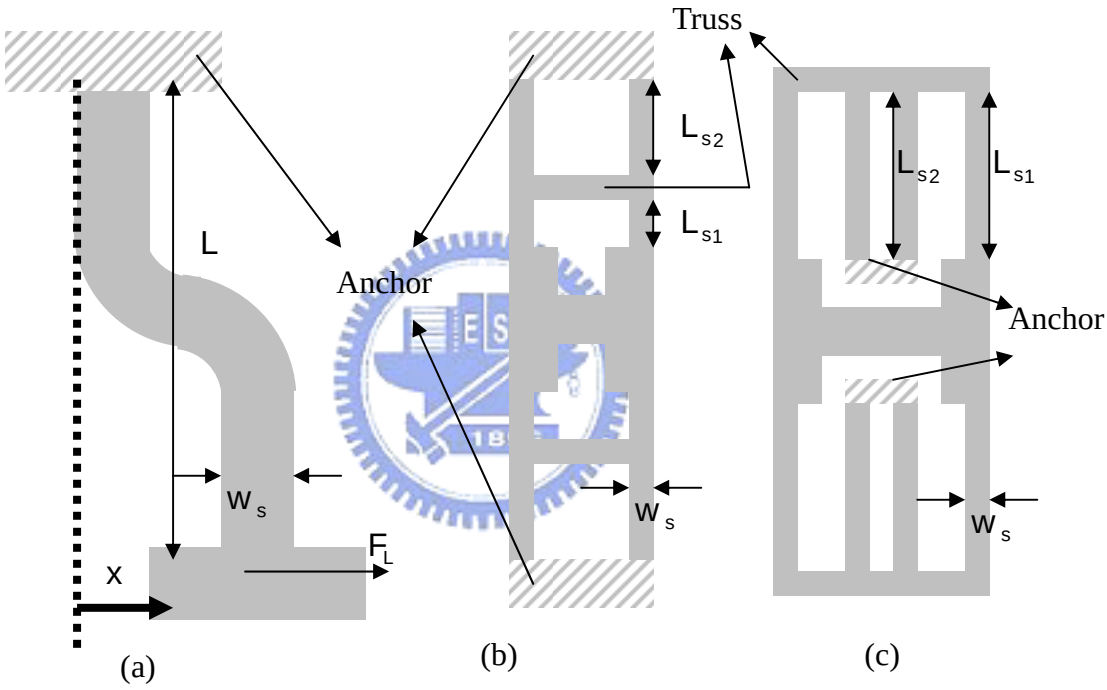

Fig 2-2 Spring structure of a (a) spring element, (b) serious connection of (a), and (c) folded structure

2-1-2 Theoretical analysis of comb actuator

For a lateral driven comb actuator (moving along the x-direction), an engaged pair of fingers, defined as one cell of a comb actuator, is shown in Fig 2-3. To

simplify the electrostatic analysis, the combs in Fig 2-3 are approximated by a parallel plate model. Three dimensional effects such as the fringing field, comb-finger end effects and ground-plane levitation effects are ignored.

The capacitance between the fixed and movable comb fingers can be expressed as:

$$C = \frac{2n\varepsilon_0 t(x + L_0)}{g} \qquad (2\text{-}3)$$

where n is the number of fingers of one side, ε_0 is the dielectric constant of air, which is 8.85×10^{-12} F/m, t is the thickness of the comb fingers, L_0 is the initial comb finger overlap, x is the comb finger lateral displacement and g is the gap spacing between the fingers. The lateral electrostatic force in the x-direction for a constant applied voltage V is equal to the derivative of the electrostatic energy with respect to x:

$$F_x = \frac{1}{2}\frac{\partial C}{\partial x}V^2 = \frac{n\varepsilon_0 t}{g}V^2 \qquad (2\text{-}4)$$

According to Eq 2-4, in order to obtain a large force while keeping a relative low applied voltage, n and t should be large and the gap g should be small.

Additionally, there is an elastic force of the suspension beam along x-direction to pull the movable fingers back. When the net electrostatic force and the spring elastic force are equal, the displacement d can be expressed as [15]:

$$F_s = K_x d = F_x \Rightarrow d = \frac{n\varepsilon_0 t V^2}{2gK_x} \qquad (2\text{-}5)$$

where F_s is the elastic spring force in the x-direction and all other symbols are as previously defined. Form Eq 2-5, it can be seen that decreasing the comb gap g and increasing the electrostatic voltage will increase the static displacement.

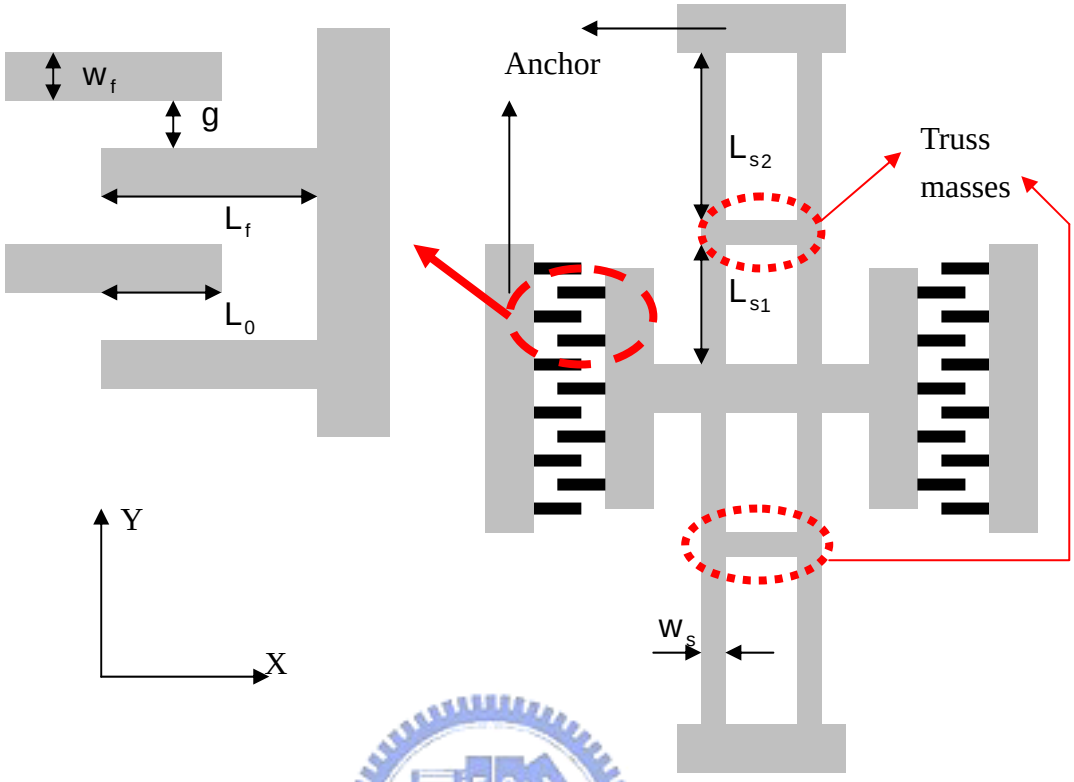

Fig 2-3 Comb drive actuator and single comb drive cell schematics

2-1-3 Resonance frequency

The optical spot scan system is to be operated in the lateral resonance mode. In the mode, the actuator can be driven to a larger displacement with lower applied voltage.

In order to calculate the resonance frequency, the actuator layout in Fig 2-3 can be modeled as a two spring mass system, as shown in Fig 2-4 [16]. The mass m_t represents the two side truss masses and the central proof mass is represented by m_c. K_c、K_t are the two side spring constants of the suspension beams L_{s1} and L_{s2}. The

lateral resonance frequency f_0 can be found to be:

$$f_0 = \sqrt{\frac{(2m_c K_t + m_t K_c) \mp \sqrt{4m_c^2 K_t^2 + m_t^2 K_c^2}}{2m_t m_r}} \qquad (2\text{-}6)$$

Note that the fundamental frequency of this system is the desired lateral resonance frequency. For a special case of equal L_{s1} and L_{s2}, K_t、K_c are equal and the frequency can be simplified to:

$$f_0 = \sqrt{\frac{K}{2m_t}(2 + \frac{m_t}{m_c} - \sqrt{4 + (\frac{m_t}{m_c})^2})} \qquad (2\text{-}7)$$

where K_t、K_c are equal to K.

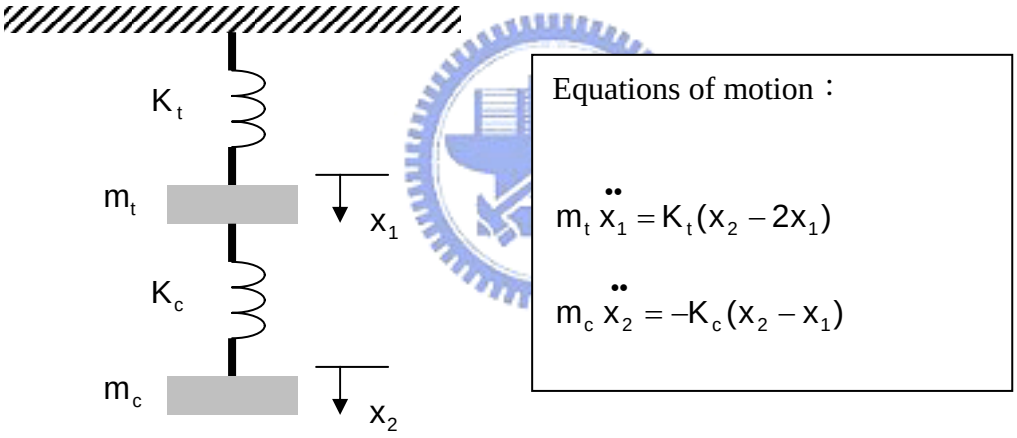

Fig 2-4 Schematic of a two degree of freedom model used to analyze the resonate frequency

2-1-4 MUMPs device in reflection type system

In the design of MUMPs comb actuator, springs with folded structures are used to reduce the layout area and residual stress. All the beam lengths are equal. The

whole actuator layout is shown in Fig 2-5. The line width and thickness are constrained by the design rules of the MUMPs process and tolerance of fabrication. Therefore, the structure thickness is 3.5μm defined by MUMPs and the finger width, spring width and gap spacing are 4μm. The width of truss mass is twice the spring width so that the full truss structure can be viewed as rigid body. The other parameters are listed in Table 2-1.

CoventorWare is used to simulate the resonance frequency by the finite element method (FEM). After meshing and calculation, first six resonance frequencies are founded and listed in Table 2-2. Fig 2-6 shows the calculated resonance mode. It can be seen that the third mode is the desired lateral mode with a resonance frequency of 26.7KHz, which is close to the theoretical analysis shown in Table 2-1.

To measure the spot profile correctly, the spot scan system should be operated in the lateral resonance mode. If other modes, such as the torsional or vertical modes, are induced, measurement error will occur, as shown in Fig 2-7. From Table 2-2, the nearest mode to the lateral mode is the vertical mode, which is spaced by 5 KHz apart. In a high-Q narrow-band resonance system, this is large enough to suppress other undesired modes.

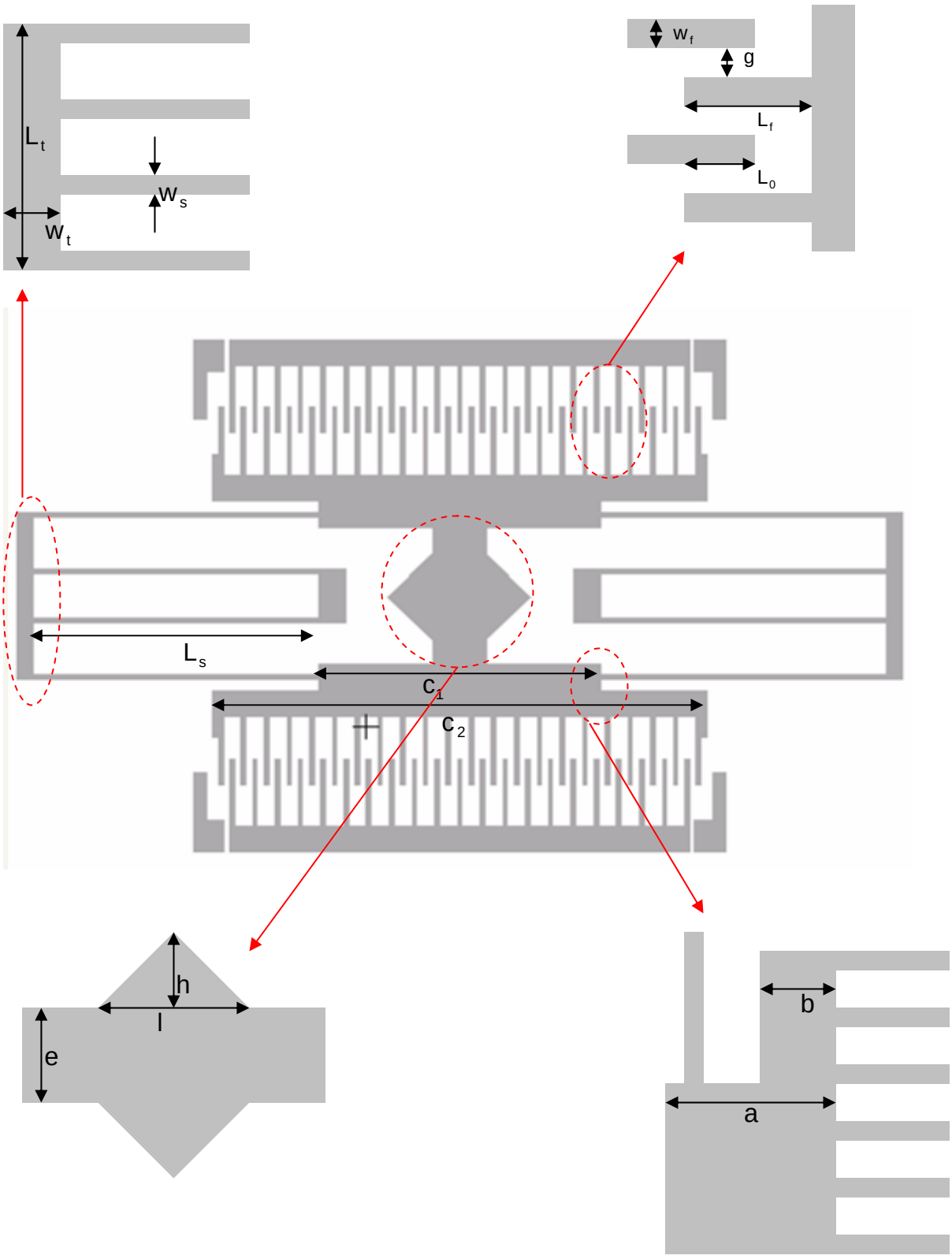

Fig 2-5 MUMPS comb actuator layout

Parameter	Dimension	Unit	Parameter	Dimension	Unit
a	40	μm	g	4	μm
b	20	μm	Thickness t	3.5	μm
c_1	200	μm	Density	2.3	g/cm^3
c_2	344	μm	Central mass m_c	2.52×10^{-10}	Kg
e	38	μm	Truss mass m_t	2.4×10^{-11}	Kg
h	31	μm	Young's modulus E	160G	Pa
l	62	μm	K_x	17.9	N/m
w_s	4	μm	f_0	29.6K	Hz
w_t	12	μm	Static displacement	0.04	μm
w_f	4	μm	at 80V d_{max}		
L_s	200	μm			
L_f	50	μm			
L_t	124	μm			
L_0	20	μm			
n	30				

Table 2-1 MUMPS comb actuator layout parameters

modeDomain

modeDomain	Frequency	Generalized Mass	Damping
1	1.850985E04	9.039082E-11	0.0
2	2.134810E04	2.215440E-10	0.0
3	2.670193E04	3.097850E-10	0.0
4	4.223982E04	7.080326E-11	0.0
5	6.607131E04	3.262059E-11	0.0
6	8.523231E04	5.527417E-11	0.0

Torsinal mode

Vertical mode

Lateral mode

Table 2-2 Mode frequencies of MUMPs device calculated by CoventorWare

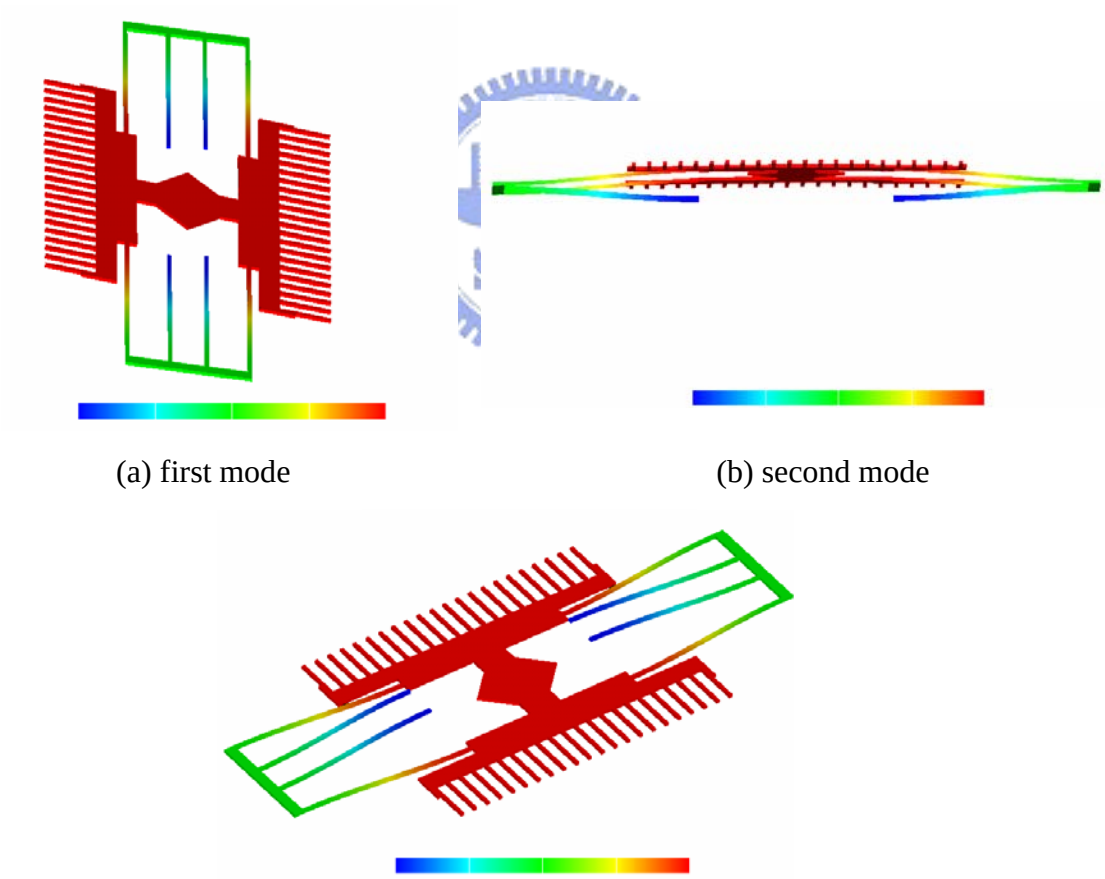

(a) first mode

(b) second mode

(c) third mode

Fig 2-6 MUMPs comb actuator mode: (a) first (torsional), (b) second (vertical), (c) third (lateral mode)

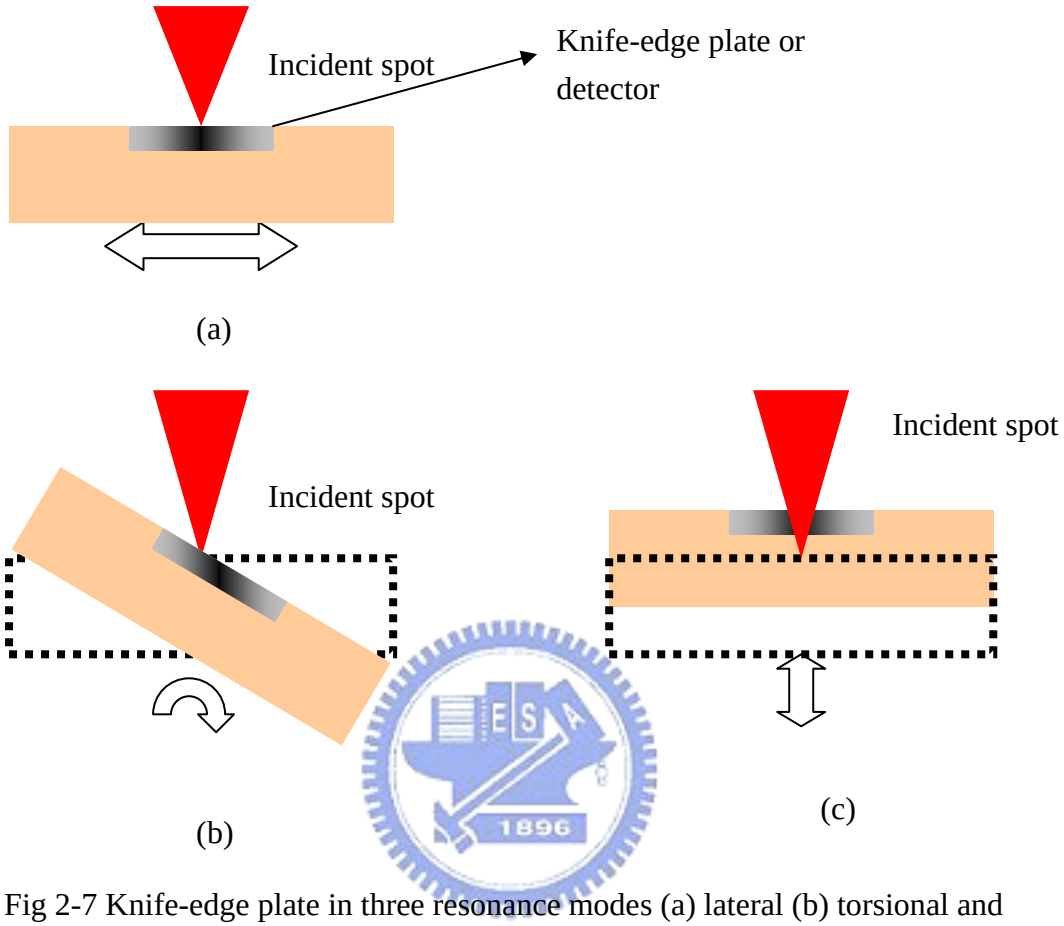

Fig 2-7 Knife-edge plate in three resonance modes (a) lateral (b) torsional and (c) vertical

2-1-5 <111> silicon substrate device in absorption type system

A similar design procedure of the MUMPs device can be adapted to design the <111> silicon device. The major difference between the two designs is the thickness. In <111> silicon substrate, the device thickness can be arbitrarily decided by ICP RIE depth. However, in order to reduce the driving voltage, the thickness is still constrained by the depth of the p-n junction [13] and chosen to 6 μm.

The folded spring design in the MUMPs device is not suitable for the <111>

silicon device due to the need to connect to the photo detector for measurement. The line width of the spring is constrained by the line width of interconnection photolithography. According to the limitations, the line width of the spring is chosen to be $6\mu m$, while the finger width and gap spacing width are the same as the MUMPs device. The width of truss mass is twice the spring width as mentioned in the MUMPs design. The layout is sown in Fig 2-8 and the other parameters and theoretical analysis in detail are shown in Table 2-3.

Fig 2-9 shows the first three modes calculated by FEM simulation. The third mode is the lateral mode with a resonance frequency of $25.5KHz$. The resonance frequencies of the first six modes are listed in Table 2-4. The frequency spacing of the lateral and the neatest next mode (torsional mode) is 5 KHz, which is large enough to separate different modes.

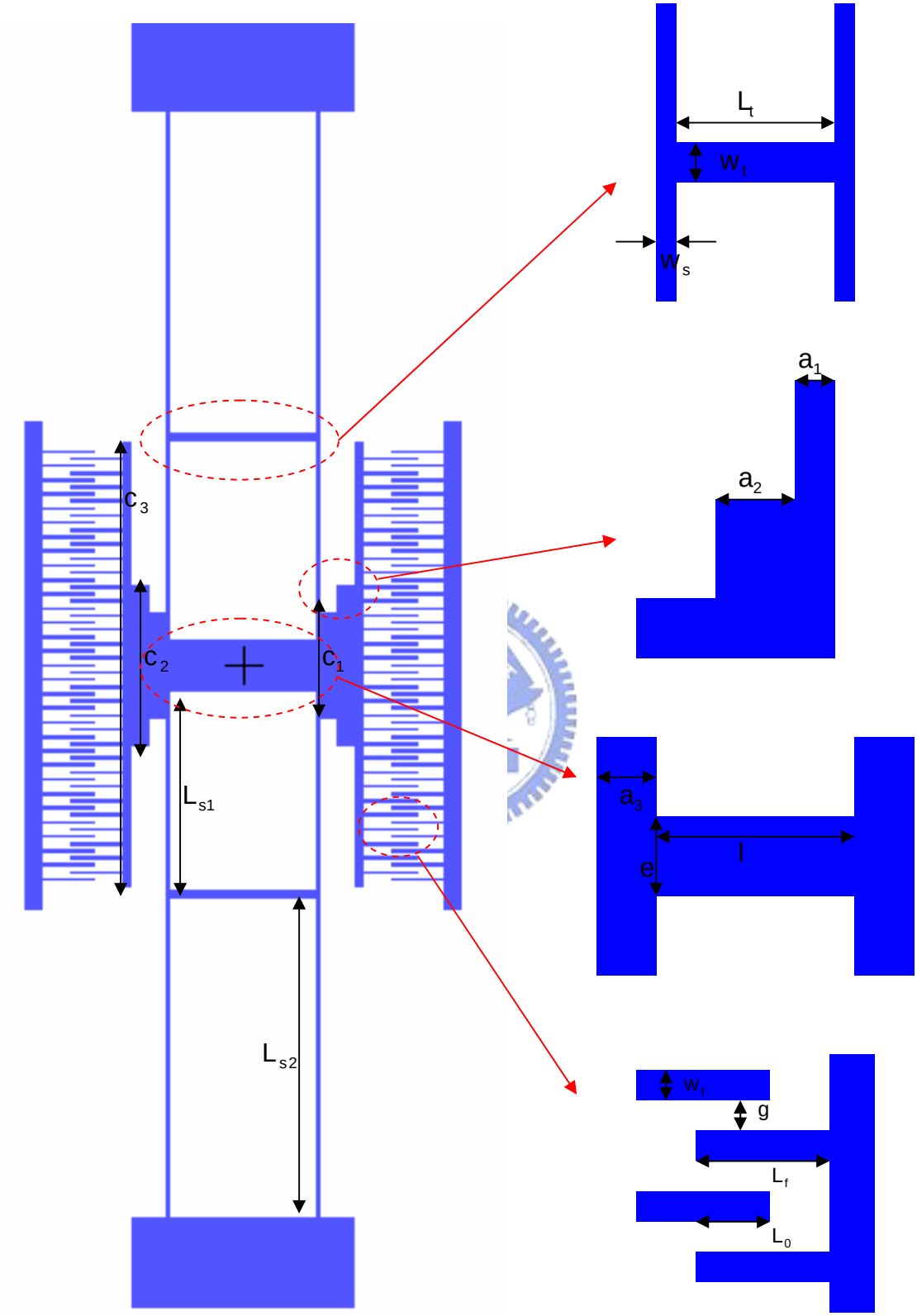

Fig 2-8 <111> silicon comb actuator layout

Parameter	Dimension	Unit	Parameter	Dimension	Unit
a_1	10	μm	g	4	μm
a_2	20	μm	Thickness t	6	μm
a_3	18	μm	Density	2.3	g/cm^3
c_1	120	μm	Central mass m_c	7.71×10^{-10}	Kg
c_2	180	μm	Truss mass m_t	5.37×10^{-11}	Kg
l	162	μm	Young's modulus E	190G	Pa
w_s	6	μm	K_t	11.5	N/m
w_t	12	μm	K_c	71.8	N/m
w_f	4	μm	K_x	40	N/m
L_{s1}	190	μm	f_0	32.4K	Hz
L_{s2}	360	μm	displacement at	0.02	μm
L_f	60	μm	80V d_{max}		
L_t	162	μm			
L_0	30	μm			
n	30				

Table 2-3 <111> silicon comb actuator layout parameters

modeDomain

modeDomain	Frequency	Generalized Mass	Damping
1	1.424612E04	7.714400E-10	0.0
2	2.027884E04	2.953520E-10	0.0
3	2.548077E04	8.275318E-10	0.0
4	4.294720E04	1.523956E-10	0.0
5	1.012226E05	1.002100E-10	0.0
6	1.323635E05	1.445391E-10	0.0

Vertical mode

Torsional mode

Lateral mode

Table 2-4 <111> silicon substrate device mode frequencies by CoventorWare

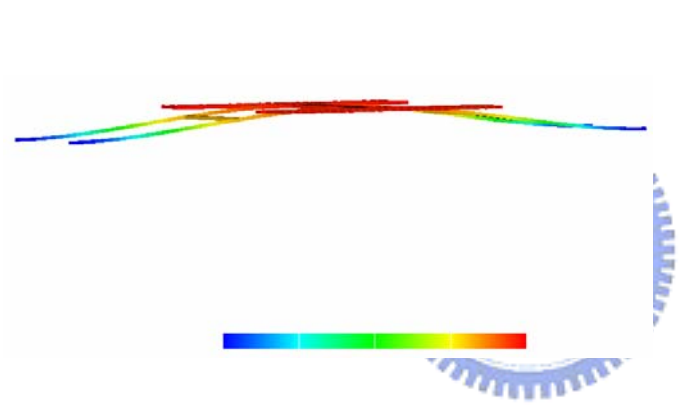

(a) first mode

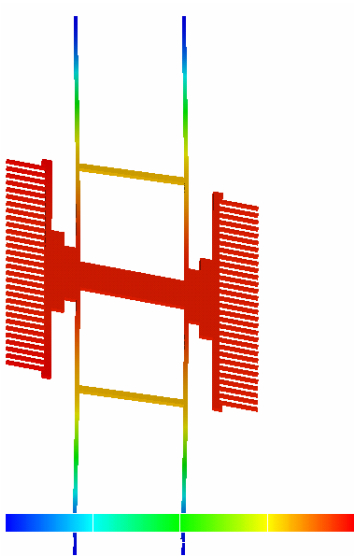

(b) second mode

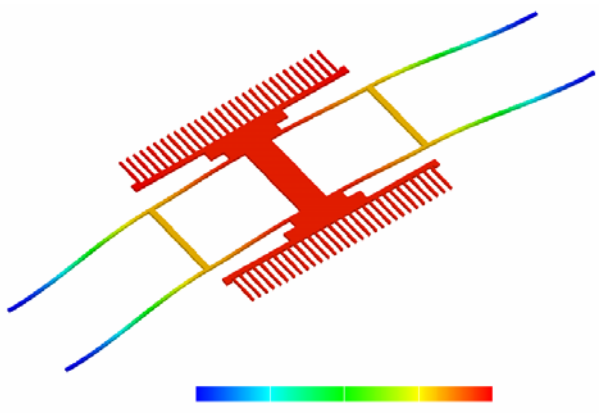

(c) third mode

Fig 2-9 <111> silicon comb actuator mode: (a) first (torsional), (b) second (vertical), (c) third (lateral mode)

2-2 Photo detector

Despite its sensible light wavelength is restricted from 100nm to 1100nm, silicon photodiodes have been widely used as standard photo detectors. This is due to its simple layout and ease to be fabricated together with other circuitries on the same chip at a low cost [17].

2-2-1 Theoretical analysis of photo detector

A simple theory for the photocurrent generation is that light absorption in the depletion region of a p-n semiconductor diode produces electron-hole pairs, which will be separated by the built-in or applied electric field. This phenomenon generates current flow in the diode. The electron-hole pairs that are generated outside the depletion region will swiftly recombine with the majority carriers and become undetectable.

Therefore, photodiode with excellent performance should be designed with a wide depletion region when a reverse bias is applied to the diode. In general, the depletion region varies with the doping profiles. A lower doping concentration and a higher resistivity in the substrate are desirable for a wider depletion region. The absorption coefficient (α) of major semiconductor materials, including silicon, are shown in Fig 2-10. For silicon, the major feature is a gradual onset of absorption above the bandgap. Owing to the indirect natural of the band structure, in contrast to a direct gap material in which the onset of absorption is much more abrupt. This causes the absorption length ($1/\alpha$) to vary significantly with wavelength and be much larger

than that in direct gap materials in the vicinity of the bandgap. Electron-hole pairs created by the absorption process will eventually recombine with one another in the absence of electric fields. Only those carriers generated in a region of significant electric field, or close enough that they may diffuse into it, have an opportunity to be collected as photocurrent. The diffusion-based component will clearly have a much slower time-response in contrast with the field-aided transport.

Consider a photo detector with a depletion region of thickness W made in a p-type bulk silicon substrate. The photocurrent (i) induced by the incident optical power (P_{inc}) are related by the responsivity (ρ) of the photo detector. Considering the substrate as the dominate source of diffusive transport and neglecting other sources of minority carriers in the substrate [18], one can obtain

$$i = P_{inc}\rho$$
$$\rho = \frac{\eta q}{h\upsilon}(1-R)\left(\frac{1-e^{-\alpha W}}{1+\alpha L_n}\right) \qquad (2\text{-}8)$$

where $(1-e^{-\alpha W})$ is the fraction of light absorbed in the depletion width (W) of the detecting junction, R is the reflection coefficient ($R=0$ in a material with 100 % absorption), L_n is the minority carrier diffusion length for electrons in the p-type substrate, q is the electron charge, $h\upsilon$ is the photon energy, and η is the internal quantum efficiency-the fraction of absorbed photons that give rise to collected electron-hole pairs. In the absence of diffusive transport, the term (αL_n) dose not appear in Eq 2-10. Note $L_n = \sqrt{D_n \tau_n}$, where D_n and τ_n are the diffusion constant and minority carrier lifetime [18]. From Eq 2-8, better responsivity can be reached by enlarging the depletion width (W) or reducing the product of absorption coefficient and minority carrier diffusion length αL_n.

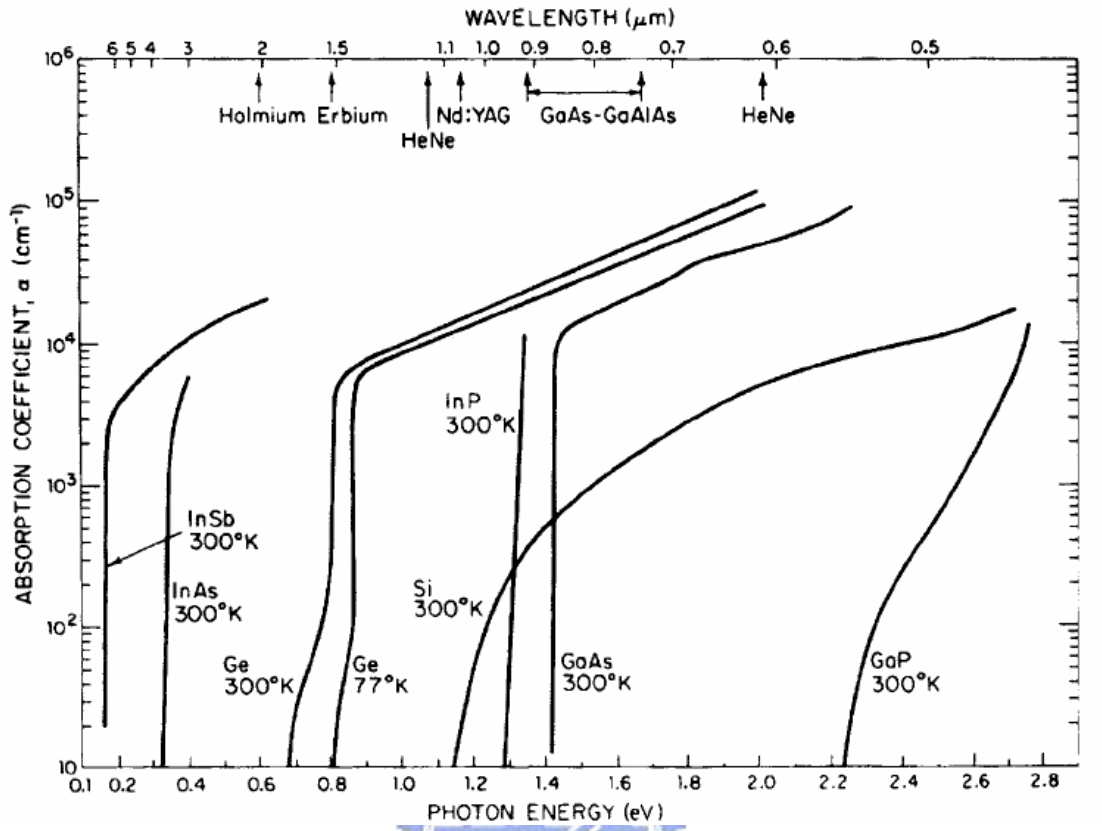

Fig 2-10 Absorption coefficient of common detector material [17]

Because the quantum mechanical process of absorption transforms a photon to an electron-hole pair regardless of the energy of the absorbed photon. Therefore, the maximum possible responsivity varies with photon energy. For example, under the assumptions of infinite depletion region, small product of absorption coefficient and minority carrier diffusion length, and no reflection ($e^{-\alpha W} \cong 0, \alpha L_n \cong 0, R = 0$), the maximum possible responsivity of red (633nm) and green (543nm) He-Ne laser can be as large as $0.51\ A/W$ and $0.44\ A/W$, respectively.

2-2-2 Photo detector design in absorption type system

In the absorption type system, the p-n junction is fabricated by ion implantation to sever as the photo detector. A heavy arsenic (As) implantation with $3\times10^{15}\ /cm^2$ dosage and 60 KeV acceleration voltage is used designed to form the N^+ region with a total doping concentration of $8\times10^{21}\ /cm^3$ in a p-type wafer with a doping concentration of $1\times10^{17}\ /cm^3$. The depletion region width w and built-in voltage V_0 can be calculated from [19],

$$w=\sqrt{\frac{2\varepsilon_0(V_0+V_b)}{qN_s}} \qquad (2\text{-}9)$$
$$V_0=\frac{kT}{q}\times\ln\left(\frac{N_s\times N_d}{2.25\times10^{25}}\right)$$

where N_s is the substrate concentration, N_d is the doping concentration, k is the Boltzmen constant, T is the absolute temperature, and V_b is the bias voltage applied to the diode. For zero bias voltage ($V_b=0$), the depletion width of the photodiode can be calculated to be $0.8\,\mu m$.

To calculate the responsivity, the diffusion length should be found first. The electron mobility is about 800 cm^2/V-sec at the substrate concentration $10^{17}\ /cm^3$, the minority diffusion lifetime is about 10^{-8} sec and the diffusion constant is 13 cm^2/sec [19], and the minority carrier diffusion length is about 4 μm ($L_n=\sqrt{D_n\tau_n}=\mu m$). From Eqs 2-7 and 2-8, for a 543nm green light laser, the responsivity of the photodiode for a bias voltage from 0 to 15V plot can be calculated and plotted as shown in Fig 2-11.

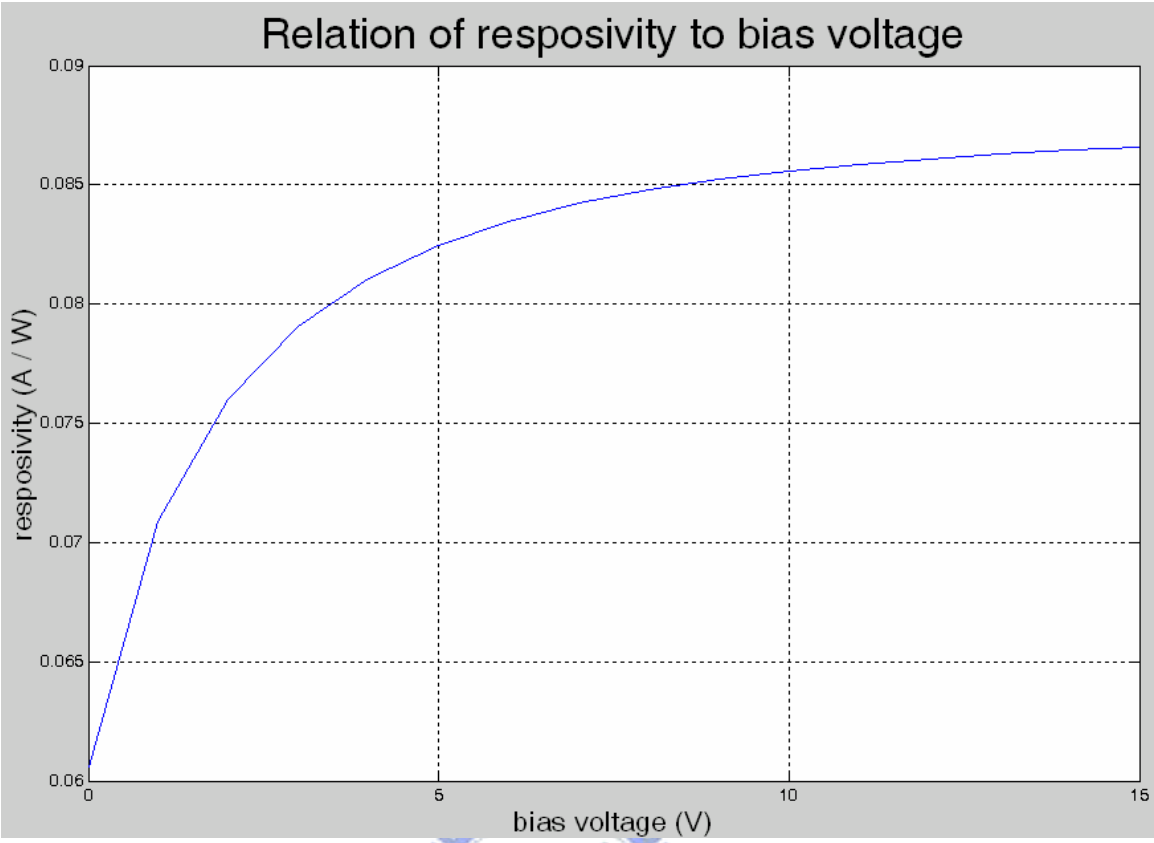

Fig 2-11 Calculated responsivity

2-3 Definition of the optical spot size

From the viewpoint of geometrical optics, light can be focused into an infinitesimal point if no aberration presented. However, the fundamental limit of optical spot size is the wave nature of light. When a uniform light passes through a finite aperture, it will be diffracted and form a diffraction pattern called Airy disk with roughly 84% energy encircled in the center ring. On the other hand, a focused light spot can usually be approximated by a Gaussian distribution, in which case the full width at half maximum (FWHM) or the full width at $1/e$ (36.8%) maximum power density is used a convenient measure of the spot size [20].

In the spot scan system, the photocurrent is proportional to the integration of the power distribution. Fig 2-12 plots the normalized power distribution and the photocurrent. For the FWHM definition, the optical spot size can be found from the photocurrent distribution between 88% and 12% of the full scale output; For the $1/e$ maximum power density definition, the optical spot size can be found from the photocurrent distribution between 92% and 8% of the full scale output the maximum output.

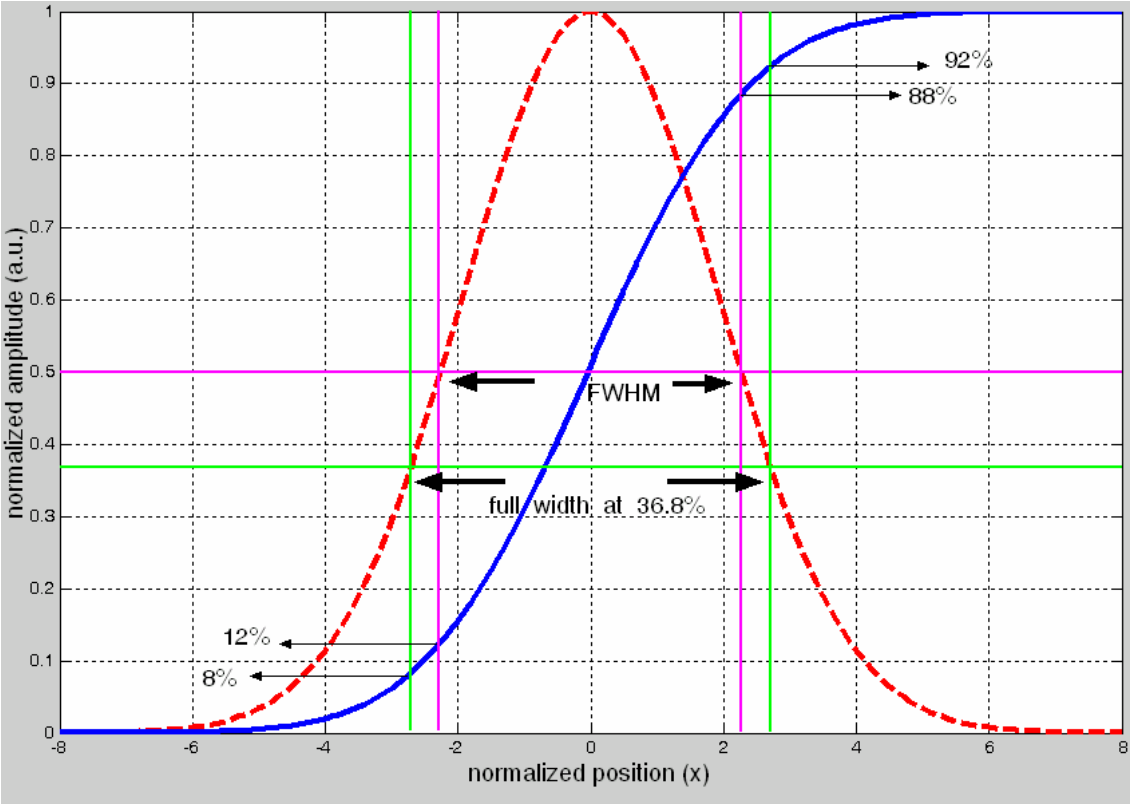

Fig 2-12 Corresponding FWHM and the full width at 36.8% definition in power and photocurrent distribution

2-4 Summary

In this chapter, the theoretical analysis of the comb actuators is conducted. The FEM simulation by CoventorWare is used to find the three major resonance modes and frequencies. The resonance frequency of the desired lateral mode is found to be far enough away from other modes to ensure proper operation of the system.

The second part shows the analysis and simulation of the photo detector of the absorption type spot scan system. In the last part, the definition of spot size and its relation to the measured photo current distribution is derived.